Published online: January 15, 2008

Molecular Systems Biology 4; Article number 157; doi:10.1038/msb4100190
Citation: ***Molecular Systems Biology*** **4:157**

www.molecularsystemsbiology.com

molecular systems biology

Probiotic modulation of symbiotic gut microbial–host metabolic interactions in a humanized microbiome mouse model

Francois-Pierre J Martin[1,2], Yulan Wang[1], Norbert Sprenger[2], Ivan KS Yap[1], Torbjörn Lundstedt[3,4], Per Lek[3], Serge Rezzi[2], Ziad Ramadan[2], Peter van Bladeren[2], Laurent B Fay[2], Sunil Kochhar[2], John C Lindon[1], Elaine Holmes[1] and Jeremy K Nicholson[1,*]

[1] Department of Biomolecular Medicine, Division of Surgery, Oncology, Reproductive Biology and Anaesthetics, Faculty of Medicine, Imperial College London, London, UK, [2] Nestlé Research Center, Lausanne, Switzerland, [3] AcurePharmaAB, Uppsala, Sweden and [4]Department of Medicinal Chemistry, BMC, Uppsala University, Uppsala, Sweden.
* Corresponding author. Department of Biomolecular Medicine, Division of Surgery, Oncology, Reproductive Biology and Anaesthetics, Faculty of Medicine, Imperial College London, Sir Alexander Fleming Building, South Kensington Campus, London SW7 2AZ, UK.
Tel.: +44 20 7594 3195; Fax: +44 20 7594 3226;
E-mail: j.nicholson@imperial.ac.uk

Received 29.6.07; accepted 17.10.07

The transgenomic metabolic effects of exposure to either *Lactobacillus paracasei* or *Lactobacillus rhamnosus* probiotics have been measured and mapped in humanized extended genome mice (germ-free mice colonized with human baby flora). Statistical analysis of the compartmental fluctuations in diverse metabolic compartments, including biofluids, tissue and cecal short-chain fatty acids (SCFAs) in relation to microbial population modulation generated a novel top-down systems biology view of the host response to probiotic intervention. Probiotic exposure exerted microbiome modification and resulted in altered hepatic lipid metabolism coupled with lowered plasma lipoprotein levels and apparent stimulated glycolysis. Probiotic treatments also altered a diverse range of pathways outcomes, including amino-acid metabolism, methylamines and SCFAs. The novel application of hierarchical-principal component analysis allowed visualization of multicompartmental transgenomic metabolic interactions that could also be resolved at the compartment and pathway level. These integrated system investigations demonstrate the potential of metabolic profiling as a top-down systems biology driver for investigating the mechanistic basis of probiotic action and the therapeutic surveillance of the gut microbial activity related to dietary supplementation of probiotics.
Molecular Systems Biology 15 January 2008; doi:10.1038/msb4100190
Subject Categories: metabolic and regulatory networks; microbiology and pathogens
Keywords: metabonomics; microbiome; NMR spectroscopy; probiotics; UPLC-MS

Introduction

The gut microbiome–mammalian 'Superorganism' (Lederberg, 2000) represents a level of biological evolutionary development in which there is extensive 'transgenomic' modulation of metabolism and physiology that is a characteristic of true symbiosis. By definition, superorganisms contain multiple cell types, and the coevolved interacting genomes can only be effectively studied as an *in vivo* unit *in situ* using top-down systems biology approaches (Nicholson, 2006; Martin *et al*, 2007a). Interest in the impact of gut microbial activity on human health is expanding rapidly and many mammalian–microbial associations, both positive and negative, have been reported (Dunne, 2001; Verdu *et al*, 2004; Nicholson *et al*, 2005; Gill *et al*, 2006; Ley *et al*, 2006). Mammalian–microbial symbiosis can play a strong role in the metabolism of endogenous and exogenous compounds and can also be influential in the etiology and development of several diseases, for example insulin resistance (Dumas *et al*, 2006), Crohn's disease (Gupta *et al*, 2000; Marchesi *et al*, 2007), irritable bowel syndrome (Sartor, 2004; Martin *et al*, 2006), food allergies (Bjorksten *et al*, 2001), gastritis and peptic ulcers (Warren, 2000; Marshall, 2003), obesity (Ley *et al*, 2006; Turnbaugh *et al*, 2006), cardiovascular disease (Pereira and Gibson, 2002) and gastrointestinal cancers (Dunne, 2001). Activities of the diverse gut microbiota can be highly specific and it has been reported that the establishment of *Bifidobacteria* is important for the development of the immune system and

Published online: January 15, 2008

for maintaining gut function (Blum and Schiffrin, 2003; Salminen *et al*, 2005; Ouwehand, 2007). In particular, elevated counts in *Bifidobacterium* with reduced *Escherichia coli*, streptococci, *Bacteroides* and clostridia counts in breast-fed babies compared to formula-fed neonates may result in the lower incidence of infections, morbidity and mortality in breast-fed infants (Dai *et al*, 2000; Kunz *et al*, 2000). As the microbiome interacts strongly with the host to determine the metabolic phenotype (Holmes and Nicholson, 2005; Gavaghan McKee *et al*, 2006) and metabolic phenotype influences outcomes of drug interventions (Nicholson *et al*, 2004; Clayton *et al*, 2006), there is clearly an important role of understanding these interactions as part of personalized healthcare solutions (Nicholson, 2006).

One of the current approaches used to modulate the balance of intestinal microflora is based on oral administration of probiotics. A probiotic is generally defined as a 'live microbial feed supplement which beneficially affects the host animal by improving its intestinal microbial balance' (Fuller, 2004). The gastrointestinal system is populated by potentially pathogenic bacteria that are capable of degrading proteins (putrefaction), releasing ammonia, amines and indoles, which in high concentrations can be toxic to humans (Cummings and Bingham, 1987). Probiotic supplementation aims at replacing or reducing the number of potentially harmful *E. coli* and *Clostridia* in the intestine by enriching the populations of gut microbiota that ferment carbohydrates and that have little proteolytic activity. Probiotics, most commonly *Lactobacillus* and *Bifidobacteria*, can be used to modulate the balance of the intestinal microflora in a beneficial way (Collins and Gibson, 1999). Although Lactobacilli do not predominate among the intestinal microflora, their resistance to acid conditions and bile salts toxicity results in their ubiquitous presence throughout the gut (Corcoran *et al*, 2005), hence they can exert metabolic effects at many levels. Fermented dairy products containing *Lactobacillus* have traditionally been used to modulate the microbial ecology (Dunne, 2001). In particular, *L. paracasei* was shown to modulate the intestinal physiology, to prevent infection of pathogenic bacteria (Sarker *et al*, 2005), to stimulate the immune system (Ibnou-Zekri *et al*, 2003), and to normalize gastrointestinal disorders (Martin *et al*, 2006). *L. rhamnosus* is also a significant probiotic strain with proven health benefits and therapeutic applications in the treatment of diarrhea (Szynanski *et al*, 2006), irritable bowel syndrome (Kajander *et al*, 2005), atopic eczema (Corcoran *et al*, 2005) and the prevention of urinary tract infections (Reid and Bruce, 2006). However, the functional effects of probiotic interventions cannot be fully assessed without probing the biochemistry of the host at multiple compartmental levels, and we propose that top-down systems biology provides an ideal approach to further understanding in this field. The microbiota observed in human baby flora (HBF) mice have a number of similarities with that found in formula-fed neonates (Mackie *et al*, 1999), which makes it to be a well-adapted and simplified model to assess probiotics impact on gut microbial functional ecosystems (in particular on metabolism of *Bifidobacteria* and potential *pathogens*) and subsequent effects on host metabolism.

Metabolic profiling using high-density data generating spectroscopic techniques, in combination with multivariate mathematical modelling is a tool which is well suited to generate metabolic profiles that encapsulate the top-down system response of an organism to a stressor or intervention (Nicholson and Wilson, 2003). Multivariate metabolic profiling offers a practical approach to measuring the metabolic endpoints that link directly to whole system activity and which are determined by both host genetic and environmental factors (Nicholson *et al*, 2005). Recently, metabolic profiling strategies have been successfully applied to characterizing the metabolic consequences of nutritional intervention (Rezzi *et al*, 2007; Wang *et al*, 2007) the effects of the gut microflora on mammalian metabolism (Martin *et al*, 2006, 2007a, b) and mechanisms of insulin-resistance (Dumas *et al*, 2006). In the current study, ^{1}H nuclear magnetic resonance (NMR) spectroscopy and targeted ultra performance liquid chromatography-mass spectrometry (UPLC-MS) analysis have been applied to characterize the global metabolic responses of humanized microbiome mice subsequently exposed to placebo, *Lactobacillus paracasei* or *Lactobacillus rhamnosus* supplementation. Correlation of the response across multiple biofluids and tissue, using plasma, urine, fecal extracts, liver tissues and ileal flushes as the biological matrices for the detection of dietary intervention, generates a top-down systems biology view of the response to probiotics intervention.

Results

Gut bacterial composition

Microbiological analyses were performed on fecal samples to assess the growth of the HBF in germ-free mice and to ascertain the effects of probiotics on the development of gut bacteria. The measured terminal composition of the fecal microbiota is detailed in Table I, where the statistically significant differences between the various groups were calculated using a two-tailed Mann–Whitney test. The bacterial populations of *Bifidobacteria longum* and *Staphylococcus aureus* were reduced after introduction of both probiotics. Additionally, unique effects of *L. rhamnosus* supplementation caused decreased populations of *Bifidobacterium breve, Staphylococcus epidermidis* and *Clostridium perfringens* but an increase of *E. coli*.

Gut levels of short-chain fatty acids

Short-chain fatty acids (SCFAs), namely acetate, propionate, isobutyrate, *n*-butyrate and isovalerate, were identified and quantified from the cecal content using GC-FID. The results, presented in Table II, are given in μmol per gram of dry fecal material and as mean ± s.d. for each group of mice. The production of some of the SCFAs, that is, acetate and butyrate, by the HBF mice supplemented with both of the probiotics was reduced. In addition, increases of the concentrations in isobutyrate and isovalerate were observed in the mice fed with *L. paracasei*.

Analysis of ^{1}H NMR spectroscopic data on plasma, urine, liver and fecal extracts

A series of pairwise O-PLS-DA models of ^{1}H NMR spectra were performed to extract information on the metabolic effects of

Published online: January 15, 2008

Table I Microbial species counts in mouse feces at the end of the experiment

Groups/$\log_{10}$ CFU	HBF ($n=10$)	HBF + *L. paracasei* ($n=9$)	HBF + *L. rhamnosus* ($n=9$)
L. paracasei	—	8.5 ± 0.2	—
L. rhamnosus	—	—	7.8 ± 0.2
E. coli	9.2 ± 0.3	9.4 ± 0.3	9.8 ± 0.5**
B. breve	9.1 ± 0.2	7.78 ± 2.13	8.7 ± 0.3*
B. longum	8.2 ± 0.6	5.6 ± 1.9***	6.3 ± 0.5***
S. aureus	7.4 ± 0.3	6.3 ± 0.3***	6.6 ± 0.5***
S. epidermidis	4.8 ± 0.4	4.9 ± 1.2	4.0 ± 0.5**
C. perfringens	7.2 ± 0.3	7.0 ± 0.5	5.7 ± 1.0***
Bacteroides	10.3 ± 0.2	10.4 ± 0.2	10.1 ± 0.4

$\log_{10}$ CFU (colony-forming unit) given per gram of wet weight of feces. Data are presented as mean ± s.d. Absence of specific bacterial strains in the gut microflora is indicated by ''—''. The values for the HBF mice supplemented with probiotics were compared to HBF control mice, *, ** and *** indicate a significant difference at 95, 99 and 99.9% confidence levels, respectively.

Table II Short-chain fatty acid content in the cecum from the different groups

Amounts of SCFAs given in μmol per gram of dry feces for each group	Acetate	Propionate	Isobutyrate	Butyrate	Isovalerate
HBF ($n=10$)	77.6 ± 17.6	22.3 ± 4.3	0.9 ± 0.2	3 ± 0.6	2.1 ± 0.6
HBF + *L. paracasei* ($n=9$)	52.3 ± 23.6***	22.2 ± 10.8	1.2 ± 0.5***	1.5 ± 0.8***	2.7 ± 1.2**
HBF + *L. rhamnosus* ($n=9$)	40.6 ± 8***	20.3 ± 2.8	0.8 ± 0.2	2.1 ± 0.4***	2.1 ± 0.5

Data are presented in μmol per gram of dry feces and are presented as means ± s.d. The amounts of SCFAs for the HBF mice supplemented with probiotics were compared to HBF control mice, ** and *** indicate a significant difference at 99 and 99.9% confidence levels, respectively.

probiotic modulation. A statistically significant metabolic phenotype separation between untreated mice and probiotic supplemented animals was observed as reflected by the high value of Q^2_Y for each model (Cloarec *et al*, 2005b; Table III). The corresponding coefficients describing the most important metabolites in plasma, liver, urine and fecal extracts that contributed to group separation are also listed in Supplementary Table 1. The area normalized intensities (10^1 a.u.) of representative metabolite signals are given as means ± s.d. in Table III. The O-PLS-DA coefficients plots are presented in Figure 1 using a back-scaling transformation and projection to aid biomarker visualization (Cloarec *et al*, 2005b). The direction of the signals in the plots relative to zero indicates positive or negative covariance with the probiotic-treated class. Each variable is plotted with a color code that indicates its discriminating power as calculated from the correlation matrix thus highlighting biomarker-rich spectral regions.

Liver metabolic profiles

Livers of mice fed with *L. paracasei* showed relative decreases in dimethylamine (DMA), trimethylamine (TMA), leucine, isoleucine, glutamine, and glycogen and increased levels of succinate and lactate (Figure 1A). Mice supplemented with *L. rhamnosus* showed relative decreases in leucine and isoleucine and relative increases in succinate, TMA and trimethylamine-*N*-oxide (TMAO) in the liver compared to controls (Figure 1D).

Plasma metabolic profiles

Plasma samples showed relative decreases in the levels of lipoproteins and increases in the concentrations of glycerophosphorylcholine (GPC) and triglycerides in mice fed with both probiotics compared to controls (Figure 1B and E). Elevated choline levels were observed in plasma of mice fed with *L. rhamnosus* and reduced plasma citrate levels were observed in mice fed with *L. paracasei* compared to controls.

Fecal extract metabolic profiles

Marked changes were observed in the metabolic profiles of fecal extracts from all supplemented mice, for example relative decreased concentrations of choline, acetate, ethanol, a range of putative *N*-acetylated metabolites (NAMs), unconjugated bile acids (BAs) and tauro-conjugated bile acids (Figure 1C and F). Furthermore, relative higher levels of glucose, lysine and polysaccharides were detected in the feces from mice fed with probiotics. A relative increased level of n-caproate (chemical shifts δ at 0.89(t), 1.27(m), 1.63(q), 2.34(t)) appeared to be associated with mice supplemented with *L. paracasei*.

Urine metabolic profiles

Urine samples of mice supplemented with both probiotics showed relative increased concentrations of indoleacetylglycine (IAG), phenylacetylglycine (PAG), tryptamine and a relative decrease in the levels of α-keto-isocaproate and citrate (Figure 1G and H). Relative increased concentrations of a mixture of putative glycolipids (UGLp, chemical shifts of multiplets at δ 0.89, 1.27, 1.56, 1.68, 2.15, 2.25, 3.10, 3.55, 3.60), *N*-acetyl-glycoproteins (NAGs) and a reduction in 3-hydroxy-isovalerate were also observed in mice supplemented with *L. paracasei* compared to controls. Urine of mice fed with *L. rhamnosus* showed a reduction in levels of creatine and citrulline.

Published online: January 15, 2008

Table III Summary of influential metabolites for discriminating NMR spectra of liver, plasma, fecal extracts and urine

Metabolites	Chemical shift and multiplicity	HBF controls	HBF + *L. paracsei*	HBF + *L. rhamnosus*
Liver			$Q^2_Y = 21\%$, $R^2_X = 44\%$	$Q^2_Y = 41\%$, $R^2_X = 37\%$
Leu	0.92(t)	2.4 ± 0.6	1.7 ± 0.3***	1.9 ± 0.5*
Ileu	0.94 (t)	0.8 ± 0.1	0.6 ± 0.05***	0.7 ± 0.2
Lactate	1.32(d)	38.4 ± 5.8	46.2 ± 8.2[a]	39.2 ± 9.7
Succinate	2.41(s)	0.2 ± 0.1	1.0 ± 0.6**	0.7 ± 0.3*
MA	2.61(s)	0.1 ± 0.06	0.04 ± 0.002**	0.08 ± 0.05
TMA	2.91 (s)	0.2 ± 0.04	0.07 ± 0.03***	0.2 ± 0.09
TMAO	3.27(s)	10.3 ± 2.2	13.1 ± 3.7	18.5 ± 8.0**
Gln	2.44(m)	0.4 ± 0.1	0.3 ± 0.1*	0.3 ± 0.1
Glycogen	5.38–5.45	3.4 ± 1.9	1.5 ± 0.6*	3.2 ± 1.9
Plasma			$Q^2_Y = 44\%$, $R^2_X = 50\%$	$Q^2_Y = 51\%$, $R^2_X = 32\%$
Lipoproteins	0.84 (m)	13.7 ± 1.8	10.1 ± 0.9***	9.8 ± 4.2**
Citrate	2.65(d)	1.4 ± 0.3	0.9 ± 0.4**	1.1 ± 0.2**
Choline	3.2(s)	11.6 ± 2.6	16.2 ± 5.7*	20.5 ± 3.8***
GPC	3.22(s)	44.1 ± 4.6	57.3 ± 12.5**	68.1 ± 11.2***
Glyceryls	3.91(m)	2.0 ± 0.3	2.5 ± 0.4**	2.7 ± 0.4**
Feces			$Q^2_Y = 90\%$, $R^2_X = 48\%$	$Q^2_Y = 89\%$, $R^2_X = 49\%$
Caprylate	1.27(m)	2.5 ± 0.1	3.5 ± 0.2***	2.4 ± 0.1
Lys	3.00(m)	3.2 ± 0.8	5.0 ± 0.3***	4.9 ± 1.2**
Osides	5.42(m)	0.9 ± 0.09	1.2 ± 0.1***	1.4 ± 0.1***
Bile acids	0.72(s)	3.1 ± 0.9	1.8 ± 0.7**	2.0 ± 0.6*
Ethanol	1.18(t)	2.5 ± 0.1	2.0 ± 0.08***	1.9 ± 0.09***
Choline	3.20(s)	48.0 ± 19.5	11.3 ± 4.1***	20.3 ± 10.9***
NAM	2.06(m)	7.1 ± 1.0	5.4 ± 0.3***	5.5 ± 0.3***
Acetate	1.91(s)	58.7 ± 34.2	27.0 ± 9.2**	32.9 ± 12.9*
U1	3.71(s)	9.2 ± 0.5	7.3 ± 0.3***	8.2 ± 0.5***
Urine			$Q^2_Y = 91\%$, $R^2_X = 47\%$	$Q^2_Y = 59\%$, $R^2_X = 46\%$
IAG	7.55(d)	0.1 ± 0.03	0.6 ± 0.2***	0.4 ± 0.2**
PAG	7.37(m)	0.8 ± 0.1	1.5 ± 0.3***	1.2 ± 0.4*
Tryptamine	7.70(d)	0.1 ± 0.04	0.4 ± 0.1***	0.2 ± 0.1**
UGLp	1.27(m)	1.7 ± 0.1	2.7 ± 0.4***	1.7 ± 0.2
Glycero-metabolites	4.04 (m)	1.7 ± 0.1	2.2 ± 0.2***	1.9 ± 0.2*
NAG	2.04(s)	3.5 ± 0.2	4.3 ± 0.2***	3.8 ± 0.5
Butyrate	0.90(t)	6.9 ± 0.8	5.2 ± 0.7**	5.2 ± 0.9**
α-keto-isocaproate	0.94(d)	13.8 ± 4.6	6.1 ± 2.3**	7.9 ± 2.1**
Propionate	1.05(t)	0.9 ± 0.2	0.8 ± 0.04*	0.8 ± 0.1
3-hydroxy-isovalerate	1.24(s)	3.0 ± 0.4	2.1 ± 0.4**	2.6 ± 0.2
Citrate	2.55(d)	10.8 ± 7.6	1.6 ± 0.6**	2.2 ± 0.9*
Creatine	3.92(s)	5.7 ± 2.1	4.5 ± 1.5	3.5 ± 0.3**
Citrulline	1.88(m)	3.8 ± 0.5	3.3 ± 0.4	3.0 ± 0.4**

O-PLS models were generated for comparing probiotics treated to HBF control mice using one predictive and two orthogonal components, R_X^2 value shows how much of the variation is explained, Q_Y^2 value represents the predictability of the models, and relates to its statistical validity. Data are presented as area normalized intensities (10^1 a.u.) of representative metabolite signals as means ± s.d. The values for the HBF mice supplemented with probiotics were compared to HBF control mice, [a], *, **, ** and *** indicate a significant difference at 90, 95, 99 and 99.9% confidence levels, respectively.
s, singlet; d, doublet; t, triplet; q, quartet; m, multiplet; dd, doublet of doublets. For metabolite abbreviations, refer to the key in Figure 1, MA: methylamine.

UPLC-MS analysis of bile acids in ileal flushes

The proportion of bile acids in ileal flushes from the different groups are given in Table IV and are shown as mean ± s.d. of the percentage of the total bile acid content. O-PLS-DA of the data set revealed that the relative concentrations of bile acids obtained from unsupplemented HBF mice are separated from those treated with probiotics, the correlation observed with *L. paracasei* being more significant than with *L. rhamnosus* as noted by the values of the cross-validated model parameter Q^2_Y (Figure 2). For example, HBF mice supplemented with *L. paracasei* showed strong correlations with higher amounts of GCA, CDCA and UDCA and lower levels of α-MCA in the ileal flushes when compared to controls. HBF mice fed with *L. rhamnosus* also showed higher levels of GCA associated with lower levels of TUDCA and TCDCA in the ileal flushes when compared to untreated HBF mice.

Integration of multicompartment metabolic data using hierarchical-principal component analysis

A principal component analysis (PCA) model was initially constructed separately for the metabolic data from each individual biological matrix (plasma, urine, liver, fecal extracts and bile acid composition in ileal flush; Figures 3 and 4). Three principal components were calculated for each cross-validated PCA model, except for the plasma where four principal components were retained to maximize the explained variance R^2X and the cross-validation parameter Q^2 following the standard sevenfold cross-validation method (Cloarec *et al*, 2005b). These PCA models descriptors (R^2X/Q^2) were 0.70/0.36 (plasma), 0.41/0.11 (urine), 0.80/0.71 (liver), 0.94/0.67 (bile acid) and 0.61/0.42 (feces). The score vectors $\mathbf{t}_b$ from each model were then assigned as new X-variables (Figure 3). Thus, the top level X-matrix contained 16 descriptors, denoted

Published online: January 15, 2008

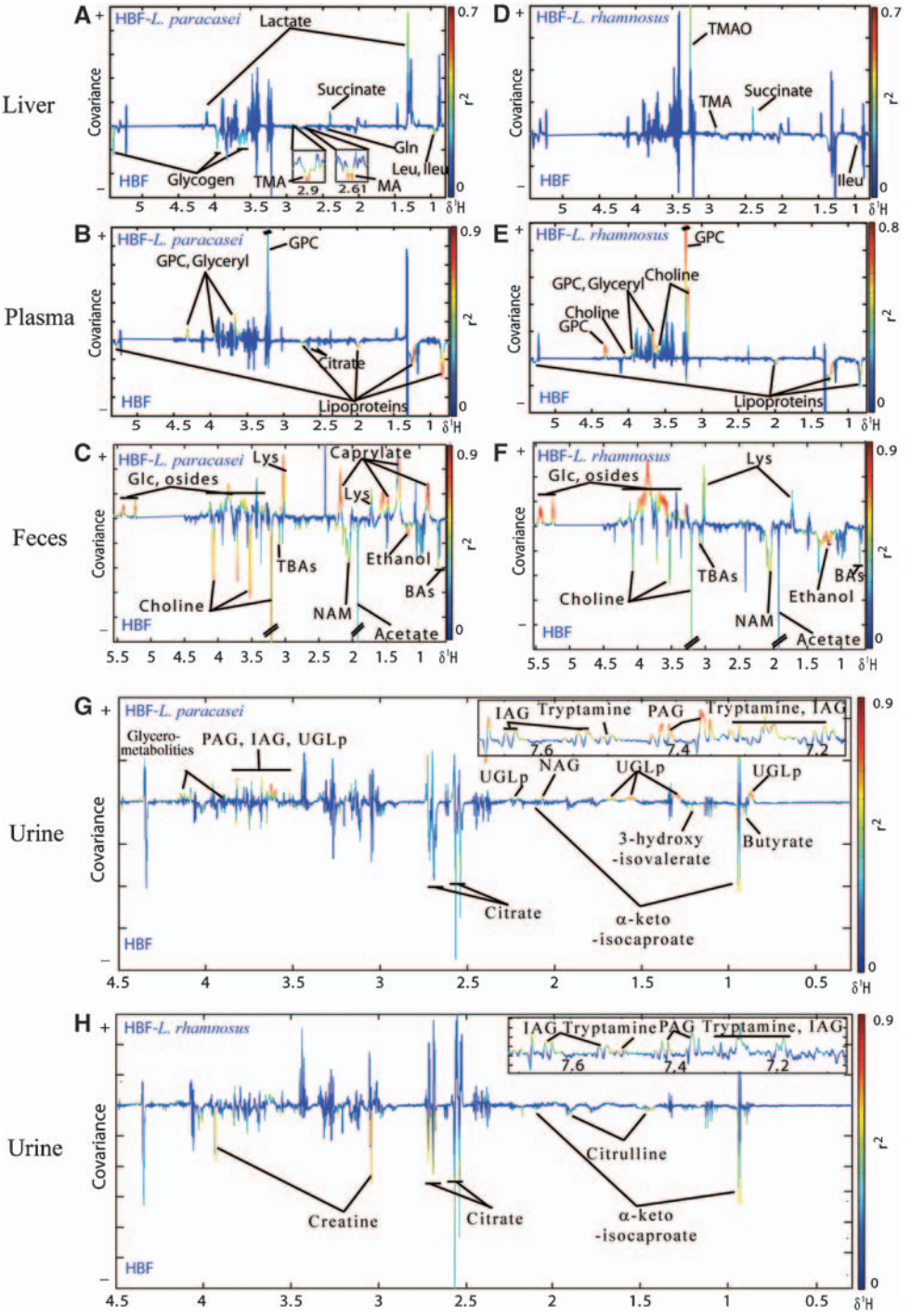

Figure 1 O-PLS-DA coefficient plots derived from ^{1}H MAS NMR CPMG spectra of liver (**A, D**), ^{1}H NMR CPMG spectra of plasma (**B, E**), ^{1}H NMR standard spectra of fecal extracts (**C, F**) and urine (**G, H**), indicating discrimination between HBF mice fed with probiotics (positive) and HBF control mice (negative). The color code corresponds to the correlation coefficients of the variables with the classes. BAs, Bile acids; DMA, dimethylamine; Glc, glucose; Gln, glutamine; GPC, glycerophosphorylcholine; IAG, indoleacetylglycine; Ileu, isoleucine; Leu, leucine; Lys, lysine; NAG, *N*-acetylated glycoproteins; NAM, *N*-acetylated metabolites; Osides, glycosides; PAG, phenylacetylglycine; TBAs, taurine conjugated to bile acids; TMA, trimethylamine; TMAO, trimethylamine-*N*-oxide; UGLp, unidentified glycolipids.

P_i (plasma PCs 1–4), L_i (liver PCs 1–3), U_i (urine PCs 1–3), B_i (bile acid PCs 1–3) and F_i (fecal PCs 1–3), which comprise only the systematic variation from each of the blocks/compartments. The two first principal components (p1 and p2) calculated for the hierarchical-principal component analysis (H-PCA; Westerhuis *et al*, 1998) model (R^2X=0.60) accounted for 37 and 23% of the total variance in the combined multi compartment data respectively. The cross validation for the H-PCA model failed due to the high degree of orthogonality within the X-matrix, that is, within each of the blocks all variables

Published online: January 15, 2008

are orthogonal to each other, while each of the biological matrices could be cross-validated at the individual level.

The H-PCA scores plot illustrated a degree of clustering with respect to the groups of HBF mice (Figure 4A). The corresponding H-PCA loadings plot indicated the contribution of the 16 descriptors to the differences observed between the samples in the H-PCA scores plot. Probiotic-supplemented HBF animals are separated from the controls along the first principal component, and this arises from the main variations modelled at the base level PCA of the individual plasma (P1, P2), liver (L2, L3), ileal flush (B2) and urine (U1, U2) data sets (Figure 4B). HBF mice fed with *L. paracasei* were separated from those fed with *L. rhamnosus* along the second principal component, which was mainly due to the variations modelled at the base level PCA of plasma (P2, P3), liver (L1) and urine (U1, U3). Interestingly, the metabolic variations in the fecal samples have no weight in discriminating the bacterial supplementation from the corresponding controls in the global model.

To uncover variables contributing to the H-PCA super scores, the loadings at the base level PCA model were interrogated (Figure 4C–F). HBF mice supplemented with probiotics showed higher concentrations of glucose, choline, GPC, glutamine, glutamate and lysine in the plasma profiles associated with elevated concentrations of glucose in the liver and higher levels of TUDCA and TCDCA in the ileal flushes. Controls showed higher levels of lipoproteins in the plasma, elevated concentrations of lipids, glycogen, glutamine, glutamate, alanine, TMAO and lactate in the liver, associated with higher levels of TCA and TβMCA in the ileal content. Unsupplemented HBF mice also showed elevated urinary excretions of creatine, citrate, citrulline, lysine, UGLp, NAG and α-keto-isocaproate compared to animals fed with probiotics. Moreover, H-PCA also revealed that HBF mice treated with *L. rhamnosus* had higher levels of hepatic lipids and plasma lipoproteins but lower concentrations of lactate and amino acids in plasma and lower urinary excretion of PAG, IAG, tryptamine and taurine than HBF mice treated with *L. paracasei*.

Table IV Bile acids composition in gut flushes for the different microbiota

Microbiota/ Bile acids	HBF	HBF + *L. paracasei*	HBF + *L. rhamnosus*
CDCA	ND	0.04 ± 0.07	0.01 ± 0.02
UDCA	ND	0.1 ± 0.1	ND
CA	0.4 ± 0.5	0.3 ± 0.7	0.3 ± 0.2
ωMCA	ND	0.02 ± 0.07	ND
αMCA	0.3 ± 0.2	0.3 ± 0.6	0.2 ± 0.2
βMCA	0.9 ± 0.7	1.3 ± 2.7	0.8 ± 0.7
GCA	ND	0.1 ± 0.1	0.1 ± .08
TCDCA	3.3 ± 1	4 ± 2.1	2.5 ± 1.3
TUDC A	6.6 ± 1.4	6.6 ± 5.2	5.1 ± 1.02
TβMCA	50 ± 4.8	49.2 ± 7.5	50.5 ± 5.2
TCA	38 ± 3.5	38 ± 6.2	40.4 ± 5

Relative composition in bile acids given in percentage of total bile acid content. Species not detected with UPLC-MS experiment are shown as ND. The key is given in UPLC-MS material and methods.

Integration of correlations between bile acids and fecal flora

We further investigated the connections between fecal flora and intestinal bile acids using a correlation analysis based bipartite graphical modelling approach (see Materials and methods; Figure 5) used previously to investigate the effects of gut microbiome humanization in germfree mice (Martin *et al*, 2007a). In the current study, we are working with a superior

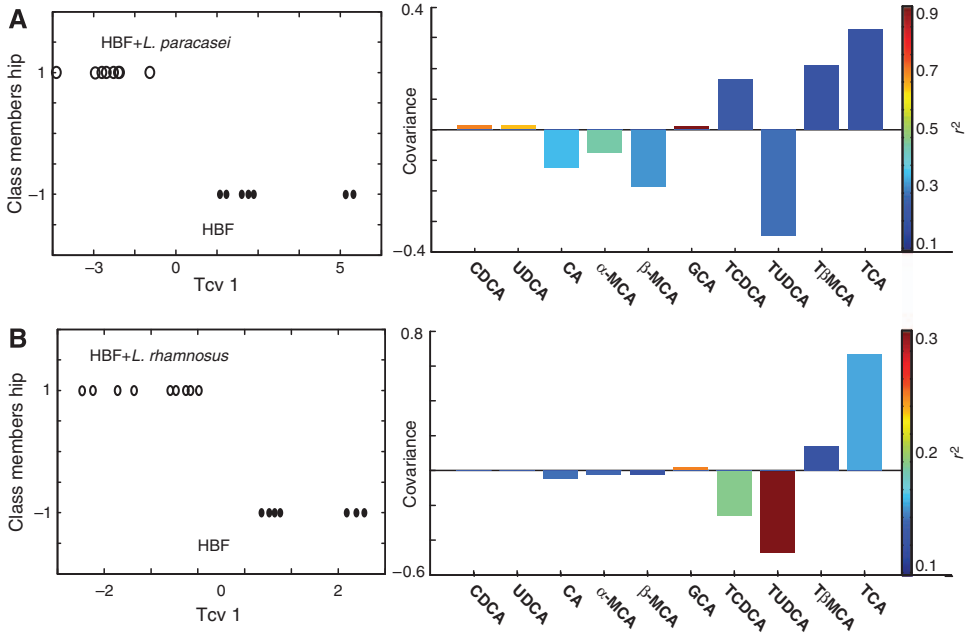

Figure 2 O-PLS-DA coefficient plots derived from the bile acid composition obtained by UPLC-MS analysis of ileal flushes, which indicate discrimination between HBF control mice (negative) and HBF mice treated with probiotics (positive), (**A**) *L. paracasei* and (**B**) *L. rhamnosus*. The color code corresponds to the correlation coefficients of the variables. One predictive and one orthogonal component were calculated; the respective Q^2_Y and R^2_X are (76.4, 52.2%) and (50.3, 51.2%).

Published online: January 15, 2008

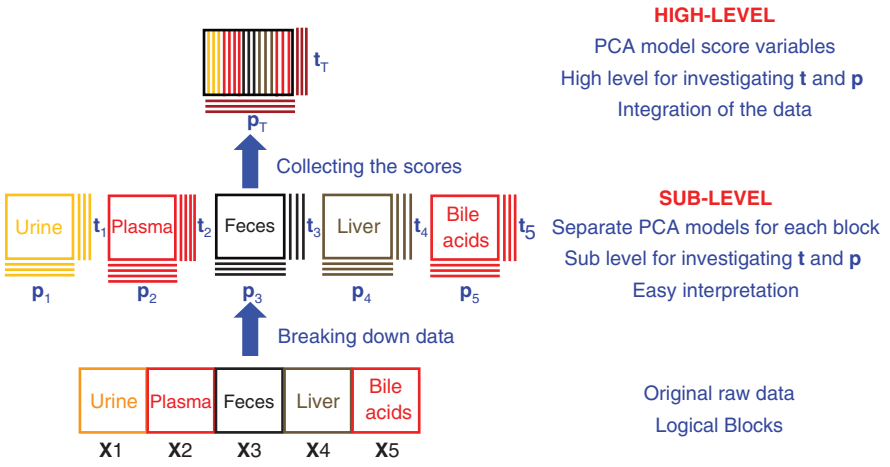

Figure 3 Schematic overview of H-PCA modelling: (Gunnarsson *et al*, 2003). In the sublevel, each block of data X*B* is modelled locally by a PCA model. Each block is summarized by one or more loading vectors $\mathbf{p}_b$ and score vectors $\mathbf{t}_p$ ('super variables'), which can be combined to form a new data matrix than can then be modelled using PCA, which generates the 'super scores' $\mathbf{t}_T$ and the 'super loadings' $\mathbf{p}_T$. All conventional PCA statistics and diagnostics are retained.

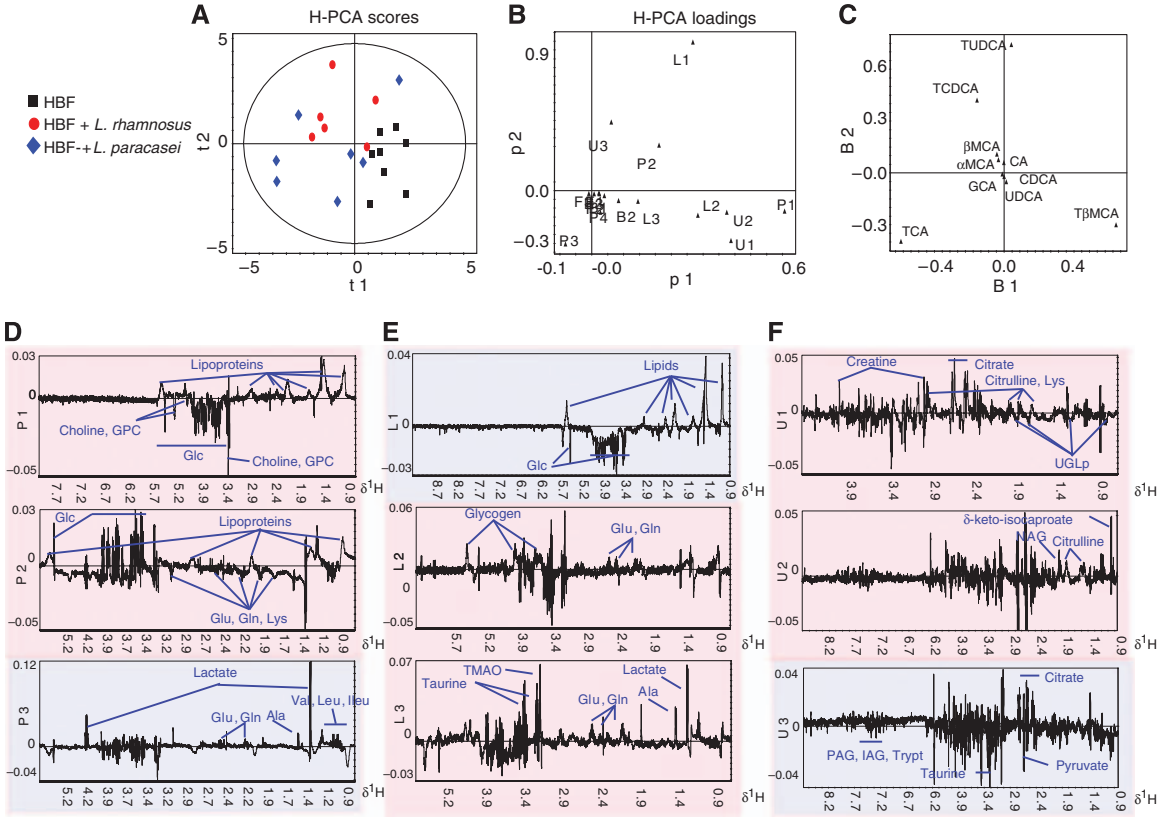

Figure 4 H-PCA scores (**A**) and loadings (**B**) plots for the two first components derived from scores of separate PCA constructed separately for the metabolic data from each individual biological matrix from HBF mice (■), HBF-*L. paracasei* mice (◆) and HBF-*L. rhamnosus* mice (○). These PCA models explained 94% (bile acid, **C**), 70% (plasma, **D**), 80% (liver, **E**), 41% (urine, **F**) and 61% (feces, data not shown) of the total variation in the data, respectively. The systematic variation from each of the block/compartment is summarized by its score vectors denoted P_i (plasma PCs 1–4), L_i (liver PCs 1–3), U_i (urine PCs 1–3), B_i (bile acid PCs 1–3) and F_i (fecal PCs 1–3), which can be combined to form a new data matrix than can then be modelled using PCA. The individual PCA loadings were color coded according to their contribution to the H-PCA model in red (principal component 1) and in blue (principal component 2). The model has been calculated from Pareto scaled data using two cross-validated PCs, R^2X=60%. Ala, alanine; see Figure 1.

model where all the major bacteria strains are identified, which was not possible when considering conventional microflora. Positive and negative correlations show the multicolinearity between bile acids and gut bacteria, whose concentrations are interdependent such as in the case of substrate–product biochemical reactions. Additional pixel maps of the correlation matrices are given to help interpretation in Supplementary Figure 1.

Published online: January 15, 2008

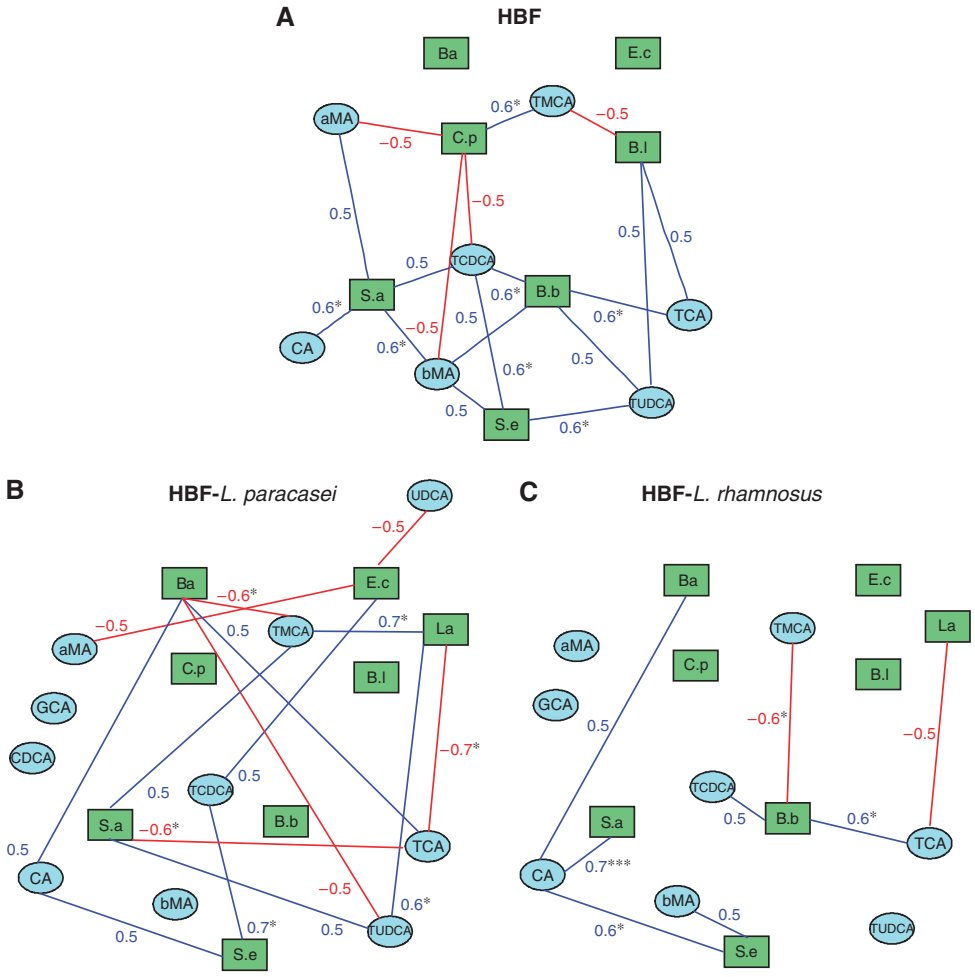

Figure 5 Integration of bile acid and fecal flora correlations. The bipartite graphs were derived from correlations between fecal flora and bile acids in each group: HBF mice (**A**), HBF mice supplemented with *L. paracasei* (**B**) or *L. rhamnosus* (**C**). The cut-off value of 0.5 was applied to the absolute value of the coefficient $|r|$ for displaying the correlations between fecal flora and bile acids. Bile acids and fecal bacteria correspond to blue ellipse nodes and green rectangle nodes, respectively. Edges are coded according to correlation value: positive and negative correlations are respectively displayed in blue and in red. aMA, α-muricholic acid; Ba, *Bacteroides*; Bb, *B. breve*; Bl, *B. longum*; bMA, β-muricholic acid; CA, cholic acid; CDCA, chenodeoxycholic acid; Cp, *C. perfringens*; Ec, *E. coli*; GCA, glycocholic acid; La, *Lactobacillus* probiotics; Sa, *S. aureus*; Se, *S. epidermidis*; TCA, taurocholic acid; TCDCA, taurochenodeoxycholic acid; TMCA, tauro-β-muricholic acid; TUDCA, tauroursocholic acid; UDCA, ursocholic acid. * and *** indicate a statistically significant correlation at 95 and 99.9% confidence levels, respectively.

Control HBF mice and HBF mice supplemented with probiotics show remarkably different bile acid/fecal flora correlation networks (Figure 5A–C), indicating that small modulations in the species composition of the microbiome can result in major functional ecological consequences. Network statistics reveal that microbiome/metabolome bipartite graphs from HBF mice supplemented with Lactobacilli show a totally different nodal structure (given for the cut-off value of 0.5). In particular, we observed that in the network obtained from control HBF mice, the most connected bacteria are Bifidobacteria, Staphylococci, and Clostridia, for which the variations are intrinsically correlated with the balance in tauro-conjugated bile acids (TCDCA, TβMCA, TCA, TUDCA) and unconjugated bile acids (CA, αMCA, βMCA). In particular, the potentially harmful opportunist *C. perfringens* shows functional correlation of opposite sign for TβMCA, TCDCA, αMCA and βMCA when compared to Bifidobacteria and *S. aureus*.

Network analysis for HBF mice supplemented with *L. paracasei* reveals that Lactobacilli supplementation resulted in decreasing the functional links between *Bifidobacteria* and bile acids, while new significant correlations were observed between bile acids, and *Bacteroides, S. aureus, S. epidermidis* and *L. paracasei*. Moreover, *E. coli* has several connections with UDCA, αMCA and TCDCA. Interestingly, *Bacteroides* shows functional correlations of opposite signs for TβMCA, TUDCA and TCA when compared to Lactobacilli and Staphylococci.

When HBF mice received *L. rhamnosus* probiotic, the microbiome/metabolome network shows a significant lower level of complexity (given for the cut-off value of 0.5). The balance within *B. breve, S. aureus* and *S. epidermidis* appears highly correlated to the composition in tauro-conjugated bile acids (TβMCA, TCA) and unconjugated bile acids (βMCA, CA).

Published online: January 15, 2008

Discussion

The cometabolic processes regulating mammalian systems and their coexisting gut microbiota are an essential evolutionary driver towards providing more refined control mechanisms on the host physiology (Pereira and Gibson, 2002; Pereira *et al*, 2003; Backhed *et al*, 2004; Holmes and Nicholson, 2005; Nicholson *et al*, 2005; Dumas *et al*, 2006; Martin *et al*, 2006, 2007a). In the present study, we demonstrate a significant association between the probiotic modulation of the gut microbiome and the metabolism of SCFAs, amino acids and methylamines, bile acids and plasma lipoproteins, and also an association with stimulated glycolysis, showing the remarkable diversity of symbiotic cometabolic connections.

Gut microbiotal links to host energy metabolism

We have recently described that HBF mice supplemented with *L. paracasei* were characterized by a high gut content of tauro-conjugated bile acids due to the inability of gut flora to deconjugate the bile acids, which resulted in high intestinal absorption of dietary lipids, accumulation of lipids in the liver and reduction of lipoprotein levels in plasma when compared to conventional animals (Martin *et al*, 2007a). Here, we show that probiotics supplementation of HBF mice resulted in a decrease in the plasma concentrations of VLDL and low-density lipoproteins (LDL) and increased triglyceride and GPC concentrations in plasma when compared to HBF controls (Figure 1B). In addition, the *Lactobacillus* supplementation resulted in decreased fecal excretion of bile acids (Figure 1C), that may be caused by accumulation of bile acids in *Lactobacillus* probiotics (Kurdi *et al*, 2000). These observation indicated probiotic-induced changes in the enterohepatic recirculation of bile acids, which were shown to lower cholesterol and systemic levels of blood lipids (Pereira and Gibson, 2002). Moreover, probiotic-specific modulation of the ileal concentrations of UDCA and CDCA (Figure 2; Table IV) may also contribute to modulation of the synthesis and secretion of VLDL into the blood (Lin *et al*, 1996; Watanabe *et al*, 2004).

Moreover, the main source of dietary lipids in animal chow is soybean oil, which is composed at 65% of long-chain polyunsaturated fatty acids. It is well known that *Lactobacillus* hydrolyzes soy oil to conjugated linoleic acid efficiently (Xu *et al*, 2005), which results in a reduction of plasma lipoprotein concentrations and hepatic cholesterol (Fukushima *et al*, 1996, 1997; Al-Othman, 2000) and in the inhibition of *S. aureus* growth (Das, 2002), as observed in the current study. Furthermore, probiotics supplementation was associated with significant reduction of acetate in the cecal content (Table II) and in a reduced hepatic acetate:propionate ratio, for which a serum lipids lowering effect has previously been described (Wong *et al*, 2006). Our results illustrate the fine relationship between a specific gut microbial population modulation and the host's lipid metabolism and that a probiotic intervention can provide refined control mechanisms on the host's physiology.

Furthermore, the molecular foundations of beneficial symbiotic host–bacteria relationships lie in the critical involvement of the microbiome in calorie recovery through further processing of dietary nutrients and indigestible fibers. Levels of leucine and isoleucine were reduced together with their keto-acid derivative (α-keto-isocaproate) in *L. paracasei*-supplemented mice. These observations suggest higher catabolism of branched-chain amino acids to produce acetyl-CoA and glucose *via* gluconeogenesis. Decreased levels of citrate in urine and plasma, but increased liver succinate levels may also indicate the shunt of the tricarboxylic acid cycle towards production of phosphoenolpyruvate for gluconeogenesis in *L. paracasei*-supplemented mice. Moreover, reduction of liver glycogen observed with *L. paracasei* supplementation is consistent with our other observations of generalized host mobilization of other metabolic fuels.

Probiotics induce specific microbiome–host transgenomic metabolic interactions

We investigated the relationship between probiotic-induced changes in gut microbes and bile acid cometabolism using bipartite graphs to display correlation patterns between fecal flora and bile acids (Figure 5). Correlation analysis derived from bile acid and fecal flora profiles offers a unique approach to capture subtle variations in bile acid composition that may be directly related to changes in gut microbial levels, and that may be induced by accumulation of bile acids in *Lactobacillus* probiotics for instance. Control HBF mice and HBF mice supplemented with probiotics show remarkably different bile acid/fecal flora correlation networks. The different bacterial strains of Bacteroides, Clostridia, Streptococci and Lactobacilli share similar abilities to deconjugate the hepatic tauro-conjugated bile acids (Midtvedt and Norman, 1967; Floch, 2002). In that regard, the overwhelming contrast between the balance of these bacteria on one hand, and conjugated bile acids (TCDCA, TβMCA, TCA, TUDCA) and unconjugated bile acids (CA, αMCA, βMCA) on the other hand, highlights the metabolic flexibility of the gut microbiota in response to probiotics supplementation. These different correlative patterns further characterize the microbial–mammalian transgenomic metabolic interactions, whereby probiotics-induced modulation of the gut microbial functional ecosystem results in different bile acid composition (Figure 2) and enterohepatic recirculation.

The relationship between specific gut microbial strains and bile acid cometabolism is well illustrated with the contrast between *Lactobacillus*, which shows resistance to bile salt toxicity (Corcoran *et al*, 2005), and *C. perfringens*, which is sensitive to the strong growth inhibitory effects of unconjugated bile acids and TCDCA (Kishinaka *et al*, 1994; Floch, 2002). In the absence of *Lactobacillus* supplementation, *C. perfringens* has anticorrelated connections with TCDCA, αMCA and βMCA, which highlights the strong inhibitory effects of these bile acids on *C. perfringens* growth. Interestingly, the probiotic supplementation was either associated with maintenance or decrease of the Clostridial population (Table I), while no functional correlations between *C. perfringens* and bile acids were observed. In that regard, these observations may indicate different nutritional competition leading to modulation of *C. perfringens* population and maintainance of the intestinal ecology. Consequently, inter-bacterial cooperation to transform bile acids is an important

Published online: January 15, 2008

factor that needs to be considered not only for the fine tuning of microbial balance but also to modulate dietary fat emulsification and absorption.

Gut-bacterial production of methylamines via choline metabolism

The elevation of methylamines (TMA, TMAO) in liver, choline and GPC in the plasma and decreased choline in feces from HBF mice supplemented with *L. rhamnosus* (Figure 1) are additional illustrations of the complex 'microbial–mammalian metabolic axis,' as the microbiota are involved in the synthesis and metabolism of these methylamines (al-Waiz *et al*, 1992). The first reaction of the methylamine pathway involves conversion of dietary choline into TMA by gut microbiota (Zeisel *et al*, 1983), which is then detoxified to TMAO in the liver *via* the flavine monooxygenase system (Smith *et al*, 1994; (Figure 6). *L. rhamnosus* supplementation contributes to higher absorption of free choline and may induce elevated production of methylamines by *Bacteroides* and *C. perfringens* (Allison and Macfarlane, 1989) through nutritional competition.

Interestingly, *L. paracasei* consumption may favor a different metabolic fate for choline through different bacterial reprocessing. Decreased fecal choline was associated with reduced concentrations of TMA and DMA in the liver, an increase in plasma GPC, but with no changes in liver TMAO and plasma choline after *L. paracasei* supplementation. These animals also showed a greater reduction in plasma lipoproteins when compared to other groups. Here, these observations may result from elevated bacterial consumption for cholesterol assimilation (Rasic, 1992) and phospholipid metabolism (Jenkins and Courtney, 2003; Taranto *et al*, 2003; Kankaanpaa *et al*, 2004). Thus, the reduced availability of choline to other bacterial strains may have led to lower production of methylamines and absorption of free choline into host metabolism.

Probiotic modulation of amino-acid metabolism

Investigation of the urine metabolic profiles showed significant increases in the concentrations of microbial cometabolites PAG, IAG and tryptamine in probiotic supplemented mice (Goodwin *et al*, 1994; Smith and Macfarlane, 1996). These metabolites are produced from amino acids, which after

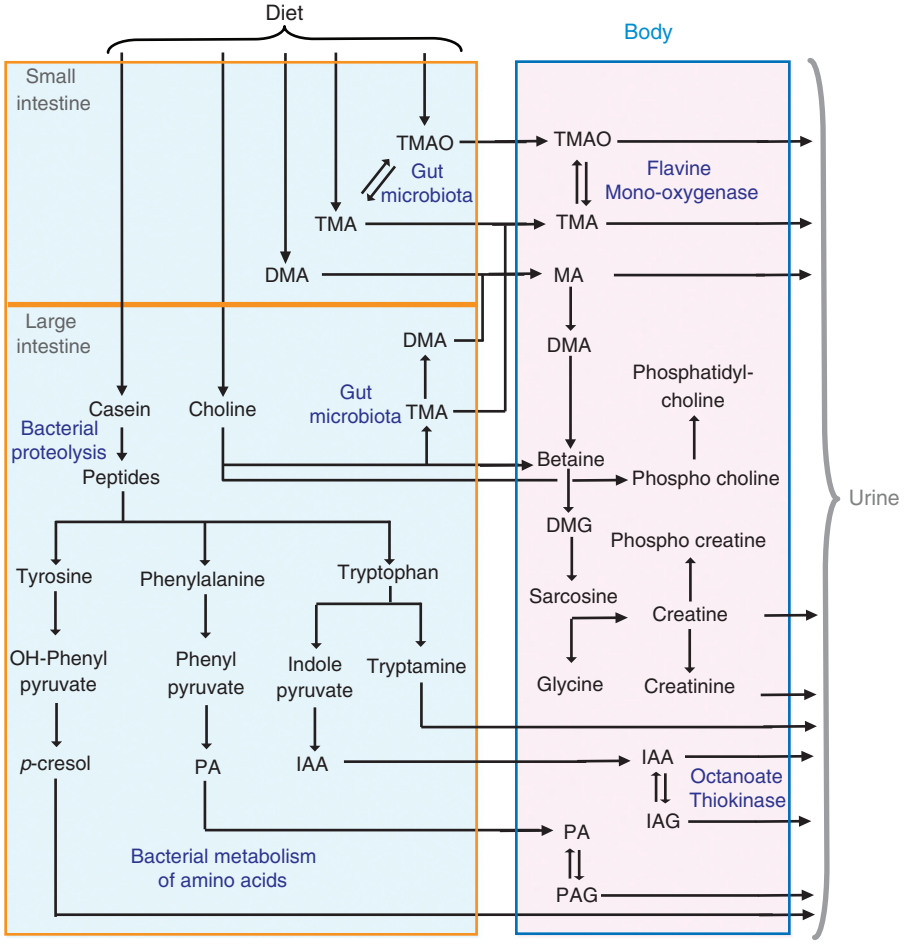

Figure 6 Gut-microbiota–mammalian cometabolism of methylamines and aromatic amino acids. DMG, dimethylglycine; IA, indoleacetate; MA, methylamine; PA, phenylacetate (see Figure 1).

Published online: January 15, 2008

depolymerization of dietary proteins (casein) by pancreatic endopeptidases and bacterial proteases and peptidases, become available for fermentation by the gut microflora (Smith and Macfarlane, 1996), as outlined in Figure 6. Metabolism of the aromatic amino acids phenylalanine, tyrosine and tryptophan generates phenylacetate (PA), *p*-cresol, indoleacetate (IA) and tryptamine, respectively (Donaldson, 1962; Smith and Macfarlane, 1996). PA and IA may be detoxified in the gut mucosa and the liver by glycine conjugation forming PAG and IAG prior to excretion *via* the urine (Donaldson, 1962; Smith and Macfarlane, 1996). The production of PA and IA has been restricted to a certain taxonomic group of gut bacteria, including *Bacteroides*, *Clostridia* and *E. coli*, which count among the dominant species in HBF colonized mice (Smith and Macfarlane, 1996; Xu *et al*, 2002). The increased urinary excretion of phenolic and indolic compounds reflects variations in gut microflora composition in relation to nutritional competition (Smith and Macfarlane, 1996; Nowak and Libudzisz, 2006). For instance, IA has been reported to inhibit the growth and survival of Lactobacilli, and specifically *L. paracasei* (Nowak and Libudzisz, 2006).

In addition, increased levels of lysine in feces from mice supplemented with probiotics is another example of bacterial contribution to the mammalian amino-acid homeostasis (Metges, 2000) and hepatic protein synthesis (Metges *et al*, 2006; Figure 1). Higher production of bacterial isobutyrate and isovalerate (Table II) suggests increased bacterial fermentation of leucine and valine that can also influence host energy metabolism (Macfarlane *et al*, 1992). Moreover, *L. paracasei* supplementation specifically induced higher urinary excretion of NAG and decreased *N*-acetylated metabolites in fecal extracts. A relationship between high casein diet and urinary excretion of NAG has been described previously (Hallson *et al*, 1997), which also suggested elevated bacterial proteolysis.

Altogether, our data suggest that the probiotic-induced increased proteolytic activities may reflect the basal metabolism of these *Lactobacillus* strains, in particular *L. paracasei* for which the proteolytic activities on casein medium are known to be elevated (Sasaki *et al*, 1995; Ikram and Mukhtar, 2006). Moreover, increased urinary NAG levels have been reported as a biomarker of increased tubular activity and tubular cell toxicity. Changes in bacterial fermentation of carbohydrates can lead to different ion absorption from the gut (Scholz-Ahrens *et al*, 2001), which may contribute to altered kidney metabolism and tubular activity. Therefore, the gut microbial contribution to the modulation of the NAG biomarker is certainly of potential toxicological assessment significance.

H-PCA modelled multicompartmental matrices related to lipid metabolism

H-PCA has been explored for the first time as a top-down systems approach to model and integrate metabolic profiles from diverse biological compartments. H-PCA modelling summarized clearly the intercorrelated changes induced by probiotic-treatment in plasma, urine and liver matrices and composition in bile acids (Figure 4). One benefit of the hierarchical approach lies in the much simplified simultaneous visualization of global system biochemical changes in multibiological matrices and improves interpretability. For instance, H-PCA resulted in a separation between the treated groups, which was not observed in separate PCA models. In addition, the H-PCA loadings plot gives the relative importance of the different blocks (biological matrices) in carrying diet-induced discriminant information. Moreover, the relationships between the descriptors in the simplified H-PCA space (H-PCA loadings plot) indicate correlations and anticorrelations between block variables, which may give insight into correlations between the metabolic variations in different biological matrices as exemplified here by metabolic changes in liver, plasma and urine and related to lipid metabolism. The H-PCA model also efficiently summarized the intercorrelated changes related to higher systemic glycolysis in plasma, urine and liver matrices, that is, reduced ketone body formation, anaerobic glycolysis, tricarboxylic cycle perturbation and amino-acid catabolism (Figure 4). Such observations might lead to better description of multiorgan metabolic perturbations (Figure 4B). This multicompartmental top-down approach offers a way forward to study the systemic biochemical profiles and regulation of function in whole organisms by analyzing simultaneously several metabolite pools from different biofluids and tissues. This approach also provides a new strategy for the quantitative and qualitative evaluation of different probiotic (or indeed any functional food or nutriceutical) interventions in relation to host biochemistry.

Conclusion

Significant associations between host metabolic phenotypes and a nutritionally modified gut-microbiota strongly supports the idea that changes across a whole range of metabolic pathways are the product of extended genome perturbations that can be oriented using probiotic supplementation, and which may play a role in host metabolic health. Bipartite network analysis highlights the metabolic flexibility of the gut microbiota, whereby bacterial strains communicate with each other to metabolize differently bile acids in a gut microbial ecosystem modulated with probiotics. In this case, probiotic consumption exerted a modification over the microbiome resulting in different hepatic influx and efflux of fatty acids in the liver, as observed with increased enterohepatic recycling of bile acids and dietary fats, lowered plasma lipoprotein levels and stimulated glycolysis. Probiotics also induced a different microbial proteolytic activity as well as modulation of bacterial metabolism of amino acids, methylamines and SCFAs. We showed the novel application of H-PCA as a means to study perturbation of metabolic profiles triggered by symbiotic microbiota at a 'global system' level by analyzing several metabolite pools simultaneously from different biofluids and tissues. These integrated system investigations demonstrate the potential of metabolic profiling as a top-down systems biology driver for investigating the mechanistic basis of probiotic action and the therapeutic surveillance of the gut microbial activity related to dietary supplementation of probiotics and their health consequences.

Published online: January 15, 2008

Materials and methods

Animal handling procedure

All animal studies were carried out under appropriate national guidelines at the Nestlé Research Center (Lausanne, Switzerland). The HBF is constituted of a total of seven bacterial strains, isolated from stool of a 20-day-old female baby that was naturally delivered and breast-fed, namely *E. coli*, *B. breve* and *B. longum*, *S. epidermidis* and *S. aureus*, *C. perfringens* and *Bacteroides distasonis*. Bacterial cell mixtures contain approximately 10^{10} cells/ml for each strain and were kept in frozen aliquots until use. *Lactobacillus paracasei* NCC2461 and *L. rhamnosus* NCC4007 probiotics were obtained from the Nestlé Culture Collection (Lausanne, Switzerland).

A total of 28 female germ-free mice (C3H strain), aged 6 weeks, received a single dose of HBF bacteria mixture and will be called HBF mice in the current manuscript. The experimental design is detailed in Supplementary Figure 2. The animals were fed with a standard pathogen-free rodent diet constituted of 50% cornstarch, 20% casein, 10% sucrose, 7% soybean oil, 5% cellulose, 0.25% choline bitartrate, 0.3% cystine and vitamin and mineral mixtures (Reeves *et al*, 1993) for 2 weeks. A control group of HBF mice (n=10) received a saline drink *ad libitum* containing Man, Rogosa and Sharpe (MRS) culture medium and was fed with a basal mix diet containing in composition 2.5% of a glucose–lactose mixture (1.25% each) for 2 additional weeks. Two groups of HBF mice were given a daily probiotic supplement, either *L. paracasei* (group A, n=9) or *L. rhamnosus* (group D, n=9), containing around 10^8 probiotic bacteria in MRS per day mixed with the saline solution *ad libitum* and were also fed with the basal mix diet.

Fecal pellets were first collected in the morning for microbiological analysis and frozen at −80°C for NMR spectroscopic analysis. Urine was then collected from animals prior to euthanasia and frozen at −80°C. Urine samples were not obtained for every animal, as some mice had an empty bladder at the time of killing (group A, n=8; group B, n=6; group C, n=8). Blood (400 μl) was collected into Li-heparin tubes and plasma was obtained after centrifugation and frozen at −80°C. The ileum and liver were dissected and snap-frozen. Ileal flush samples were obtained by rinsing the ileal lumen using a 1 ml sterile syringe containing a phosphate buffer solution (0.2 M Na_2HPO_4/0.04 M NaH_2PO_4, pH 7.4) for UPLC-MS analysis. Cecal content was collected upon animal autopsy, snap-frozen immediately and maintained at −80°C prior to analysis.

Microbial profiling of fecal contents

Immediately after collection, fecal pellets were homogenized in 0.5 ml Ringer solution (Oxoid, UK) supplemented with 0.05% (w/v) L-Cystein (HCl). The enumeration of specific microorganisms was performed after plating and incubation of different dilutions of the bacterial solution on selective and semiselective media, for example, *Bifidobacteria* on Eugom Tomato medium, *Lactobacillus* on MRS + antibiotic (phosphomycine, sulfamethoxazole, trimethoprim) medium, *C. perfringens* on NN-agar medium, *Enterobacteriaceae* on Drigalski medium and *Bacteroides* on Shaedler Neo Vanco medium. *Enterobacteriaceae* cultures were incubated at 37°C under aerobic conditions for 24 h, and other cultures were incubated under anaerobic conditions over a 48 h period.

Gas-chromatography on cecal content

An aliquot of cecal content was extracted with 4 ml buffer (0.1% (w/v) $HgCl_2$ and 1% (v/v) H_3PO_4 supplemented with 0.045 mg/ml 2,2-dimethylbutyric acid (as internal standard) per gram fresh weight. The resulting slurry was centrifuged for 30 min at 5000 *g* at 4°C. Fecal SCFAs were analyzed using a gas-chromatograph (HP 6890) equipped with a flame ionization detector and a DB-FFAP column (J&W Scientific, MSP Friedli & Co, Switzerland) of 30 m length, 530 μm diameter and 1 μm film thickness. The system was run with helium gas at an inlet constant pressure of 10 psi at 180°C. Each sample run was preceded with a cleaning injection of 1.2% formic acid. Samples were run at an initial temperature of 80°C for 1.2 min followed by heating to 145°C in 6.5 min, heating to 200°C in 0.55 min and an additional 0.5 min at 200°C. SCFAs were identified using external standards (acetate, propionate, iso-butyrate, *n*-butyrate, iso-valerate, *n*-valerate) and the concentration was calculated using the internal standard.

^{1}H NMR spectroscopic analysis

A volume of 100 μl of blood plasma was added to 450 μl of saline solution containing 10% D_2O, which was used as a spectrometer field frequency lock, into 5 mm NMR tubes. Urine samples were prepared by mixing 20 μl of samples with 30 μl of a phosphate buffer solution containing 90% D_2O and 0.25 mM 3-trimethylsilyl-1-[2,2,3,3-$^2H_4$] propionate (TSP), which was used as chemical shift reference (δ 0.0), into 1.7 mm NMR tubes. Fecal pellets were homogenized in 650 μl of a phosphate buffer solution containing 90% D_2O and 0.25 mM TSP. The fecal samples were sonicated for 30 min at 25°C and then centrifuged at 13 000 r.p.m. for 20 min to remove particulates. The supernatants were removed and centrifuged at 13 000 r.p.m. for 10 min. A 580 μl aliquot of the fecal supernatant was then pipetted into a 5 mm NMR tube for spectroscopic analysis. Portions of intact liver samples (∼15 mg) were bathed in ice-cold 0.9% saline D_2O solution and packed into a zirconium oxide 4 mm outer diameter rotor.

^{1}H NMR spectra were acquired for each sample using a Bruker DRX 600 NMR spectrometer (Rheinstetten, Germany) operating at 600.11 MHz for ^{1}H. The instrument was equipped with a Bruker 5 mm TXI triple resonance probe maintained at 298 K for liquid samples and a standard Bruker high-resolution MAS probe under magic-angle-spinning conditions at a spin rate of 5000 Hz for intact tissues (Waters *et al*, 2000). Tissue samples were regulated at 283 K to minimize biochemical degradation.

One-dimensional (1D) ^{1}H NMR spectra were obtained from each sample using a standard solvent suppression pulse sequence (RD-90°-t1-90°-tm-90°-acquire FID) with $\mathbf{t}_m$ fixed at 100 ms and $\mathbf{t}_1$ at 3 μs (Wang *et al*, 2005). Additional spin echo Carr-Purcell-Meiboom-Gill (CPMG) spectra were acquired for plasma and liver samples using the pulse sequence (RD-90°-(t-180°-t)$_n$-acquire FID), with a spin–spin relaxation delay, 2nτ, of 160 ms for plasma and 200 ms for tissue (Meiboom and Gill, 1958). The 90° pulse length was 9.0–12 μs. A total of 128 transients were collected into 32K data points with a recycle delay (RD) of 2 s. The assignment of the ^{1}H NMR spectral peaks to specific metabolites was achieved based on the literature (Nicholson *et al*, 1995; Fan, 1996), and confirmed by 2D COrrelation SpectroscopY (COSY) (Hurd, 1990) and TOtal Correlation SpectroscopY (TOCSY) (Bax and Davis, 1985). 2D NMR spectra were acquired on selected samples. Further assignment of the metabolites was also accomplished with the use of Statistical TOtal Correlation SpectroscopY (STOCSY) on 1D spectra (Cloarec *et al*, 2005a).

UPLC-MS methods

The Ultra Performance™ liquid chromatography of ileal flushes was performed on a ACQUITY UPLC system (Waters, Milford, MA, USA) equipped with a Tof™ LCT-Premier (Waters MS Technologies, Manchester, UK) for mass detection using the method we described previously (Martin *et al*, 2007a). The same conditions were applied for analysis of the following bile acid standards: cholic (CA), taurocholic (TCA), glycocholic (GCA), deoxycholic (DCA), taurodeoxycholic (TDCA), glycodeoxycholic (GDCA), chenodeoxycholic (CDCA), taurochenodeoxycholic (TCDCA), glycochenodeoxycholic (GCDCA), lithocholic (LCA), taurolithocholic (TLCA), glycolithocholic (GLCA), ursodeoxycholic (UDCA), tauroursodeoxycholic (TUDCA), glycoursodeoxycholic (GUDCA), hyocholic (HCA), α-muricholic (αMCA), β-muricholic (βMCA), ω-muricholic (ωMCA), tauro-β-muricholic (TβMCA) and tauro-α-muricholic (TαMCA) acids. We have previously given the molecular structure, the retention time and the mass to charge ratio (and not the molecular weight as published previously) of the observed ions. Unconjugated bile acids formed a formate adduct.

Data analysis

Microbial counts and SCFAs composition in the cecum were analyzed using a two-tailed Mann–Whitney test.

Published online: January 15, 2008

^{1}H NMR spectra were corrected manually for phase and baseline distortion and referenced to the chemical shift of the CH_3 resonance of alanine at δ 1.466 for plasma and liver samples, to the TSP resonance of alanine at δ 0.0 for urine and fecal samples using XwinNMR 3.5 (Bruker Biospin, Rheinstetten, Germany). The spectra were converted into 22K data points over the range of δ 0.2–10.0 using an in-house developed MATLAB routine. The regions containing the water resonance (δ 4.5–5.19), and for urine urea resonance (δ 4.5–6.2), were removed. Chemical shift intensities were normalized to the sum of all intensities within the specified range before chemometric analysis.

UPLC-MS data were processed using the Micromass MarkerLynx™ applications manager Version 4.0 (Waters Corp, Milford, USA). The peaks of bile acids were identified by comparing the m/z ratio and retention time to the set of standard bile acids measured under the same conditions. Data were noise-reduced in both of the UPLC and MS domains using MarkerLynx standard routines. Integration of the UPLC-MS bile acid peaks was performed using ApexTrack2™. Each peak integral was expressed as a ratio to the sum of integrals of the 21 measured bile acids.

The multivariate pattern recognition techniques used in this study were based on PCA (Wold *et al*, 1987), H-PCA (Westerhuis *et al*, 1998) and the orthogonal-projection to latent structure (O-PLS) (Trygg and Wold, 2003). PCA was carried out using the SIMCA-P 11 software (Umetrics, Umeå, Sweden) in order to detect the presence of inherent similarities between metabolic profiles. Both NMR and LC-MS variables were subjected to Pareto scaling, by dividing each variable by the square root of its standard deviation. Data were visualized by means of principal component scores and loadings plots. Each point in the scores plot represents an individual biochemical profile of a sample, whereas on the loadings plot each coordinate represents a single NMR spectral region or LC-MS retention time and mass to charge ratio (m/z). Because the scores and loadings plots are complementary, biochemical components responsible for the differences between samples detected in the scores plot can be extracted from the corresponding loadings plot.

O-PLS-DA was also carried out using the method developed by Trygg *et al* (Trygg and Wold, 2003) and implemented for NMR spectral data by Cloarec *et al* (2005b) to exclusively focus on the effects of probiotic supplementation. All O-PLS-DA models were constructed using one predictive and two orthogonal components using data scaled to unit variance (i.e. by dividing each variable by its standard deviation). Here, the test for the significance of the Pearson product–moment correlation coefficient was used to calculate the cut-off value of the correlation coefficients at the level of $P<0.05$. To test the validity of the model against over-fitting, the cross-validation parameter Q^2 was computed and the standard seven-fold cross validation method was used (Cloarec *et al*, 2005b). The interpretation of the model was achieved from correlation coefficient plots that incorporated a back-transformation method such that the coefficients resembled the original structure of the NMR spectral data (Cloarec *et al*, 2005b).

H-PCA methods have been proposed in the recent literature to improve the interpretability of multiple models (Westerhuis *et al*, 1998) generated from several blocks of descriptor variables measured on the same objects (Bergman *et al*, 1998; Lundstedt *et al*, 1998; Janne *et al*, 2001). The data are divided into well-defined logical blocks X1, …, X*B* (where the index B refers to each biosample type), according to an event, instrumentation or biological compartment. A consensus direction among all the blocks is sought. Here, logical blocks were defined according to the biological nature of the samples obtained from the same animals (Figure 3). Hence, five independent blocks of variables were comprised of NMR data from plasma, liver, urine and fecal extracts as well as bile acids composition obtained by UPLC-MS. PCA was performed on each data matrix individually, and block loadings $\mathbf{p}_b$ and scores $\mathbf{t}_b$ were generated for each block (Figure 3). All block scores $\mathbf{t}_b$ were then combined into a super block T. The PCA (H-PCA) was then applied to the super block T to generate the super scores $\mathbf{t}_T$ and the super loadings $\mathbf{p}_T$. The super scores $\mathbf{t}_T$ gives the relationships between the observations and all the sources of variations. The super loadings $\mathbf{p}_T$ gives the relative importance of the different blocks XB for each principal component as well as information on the relationship/covariance between the different variables in the different compartments.

Bipartite graph representation of bile acid and fecal flora profiles

The bipartite graph (Rgraphsviz) package from *R* was used to display the correlation matrix derived from bile acid and fecal flora profiles to assess the probiotic-induced changes to the microbial-mammalian transgenomic interactions (Figure 5). Pearson's correlation coefficients were computed between bile acid variables and fecal flora variables from the same mice and a cut-off value of 0.5 was applied to the absolute value of the coefficient $|r|$ so that the bipartite graph only represents the correlations between the two types of nodes (fecal flora and bile acids) above the cut-off (Martin *et al*, 2007a). The sign of the initial correlation was then color coded (red: negative, blue: positive), and the correlation value displayed on the bipartite graph. In that context, presence of edges between two specific nodes (one of each type) reveals a functional correlation (above the cut-off) between these entities.

Supplementary information

Supplementary information is available at the *Molecular Systems Biology* website (www.nature.com/msb).

Acknowledgements

We thank Dr J Trygg for use of O-PLS code and Dr O Cloarec for providing the MATLAB tool for data analysis. We acknowledge Isabelle Rochat, Catherine Murset and Gloria Reuteler for microbiota analysis; Christine Cherbut, Marc-Emmanuel Dumas and Florence Rochat for their input and help; John Newell, Monique Julita, Massimo Marchesini, Catherine Schwartz and Christophe Maubert for their help in animal husbandry. This work received financial support from Nestle to FPM, YW and from INTERMAP (grant 5-R01-HL 71950-2) to IKSY.

References

Al-Othman AA (2000) Growth and lipid metabolism responses in rats fed different dietary fat sources. *Int J Food Sci Nutr* **51:** 159–167

al-Waiz M, Mikov M, Mitchell SC, Smith RL (1992) The exogenous origin of trimethylamine in the mouse. *Metabolism* **41:** 135–136

Allison C, Macfarlane GT (1989) Influence of pH, nutrient availability, and growth rate on amine production by *Bacteroides fragilis* and *Clostridium perfringens*. *Appl Environ Microbiol* **55:** 2894–2898

Backhed F, Ding H, Wang T, Hooper LV, Koh GY, Nagy A, Semenkovich CF, Gordon JI (2004) The gut microbiota as an environmental factor that regulates fat storage. *Proc Natl Acad Sci USA* **101:** 15718–15723

Bax A, Davis D (1985) MLEV-17-based two-dimensional homonuclear magnetization transfer spectroscopy. *J Magn Reson* **65:** 355–360

Bergman R, Johansson M, Lundstedt T, Seifert E, Aberg J (1998) Optimization of a tabletting process by sequential design and multivariate analysis. *Chemom Intell Lab Syst* **44:** 271–286

Bjorksten B, Sepp E, Julge K, Voor T, Mikelsaar M (2001) Allergy development and the intestinal microflora during the first year of life. *J Allergy Clin Immunol* **108:** 516–520

Blum S, Schiffrin EJ (2003) Intestinal microflora and homeostasis of the mucosal immune response: implications for probiotic bacteria? *Curr Issues Intest Microbiol* **4:** 53–60

Clayton TA, Lindon JC, Cloarec O, Antti H, Charuel C, Hanton G, Provost JP, Le Net JL, Baker D, Walley RJ, Everett JR, Nicholson JK (2006) Pharmaco-metabonomic phenotyping and personalized drug treatment. *Nature* **440:** 1073–1077

Cloarec O, Dumas ME, Craig A, Barton RH, Trygg J, Hudson J, Blancher C, Gauguier D, Lindon JC, Holmes E, Nicholson JK (2005a) Statistical total correlation spectroscopy: an exploratory approach for latent biomarker identification from metabolic ^{1}H NMR data sets. *Anal Chem* **77:** 1282–1289

Cloarec O, Dumas ME, Trygg J, Craig A, Barton RH, Lindon JC, Nicholson JK, Holmes E (2005b) Evaluation of the orthogonal projection on latent structure model limitations caused by chemical shift variability and improved visualization of biomarker changes in 1H NMR spectroscopic metabonomic studies. *Anal Chem* **77:** 517–526

Collins MD, Gibson GR (1999) Probiotics, prebiotics, and synbiotics: approaches for modulating the microbial ecology of the gut. *Am J Clin Nutr* **69:** 1052S–1057S

Corcoran BM, Stanton C, Fitzgerald GF, Ross RP (2005) Survival of probiotic lactobacilli in acidic environments is enhanced in the presence of metabolizable sugars. *Appl Environ Microbiol* **71:** 3060–3067

Cummings JH, Bingham SA (1987) Dietary fibre, fermentation and large bowel cancer. *Cancer Surv* **6:** 601–621

Dai D, Nanthkumar NN, Newburg DS, Walker WA (2000) Role of oligosaccharides and glycoconjugates in intestinal host defense. *J Pediatr Gastroenterol Nutr* **30** (Suppl 2)**:** S23–S33

Das UN (2002) Essential fatty acids as possible enhancers of the beneficial actions of probiotics. *Nutrition* **18:** 786

Donaldson Jr RM (1962) Excretion of tryptamine and indole-3-acetic acid in urine of rats with intestinal diverticula. *Am J Physiol* **202:** 289–292

Dumas ME, Barton RH, Toye A, Cloarec O, Blancher C, Rothwell A, Fearnside J, Tatoud R, Blanc V, Lindon JC, Mitchell SC, Holmes E, McCarthy MI, Scott J, Gauguier D, Nicholson JK (2006) Metabolic profiling reveals a contribution of gut microbiota to fatty liver phenotype in insulin-resistant mice. *Proc Natl Acad Sci USA* **103:** 12511–12516

Dunne C (2001) Adaptation of bacteria to the intestinal niche: probiotics and gut disorder. *Inflamm Bowel Dis* **7:** 136–145

Fan TW (1996) Metabolite profiling by one- and two-dimensional NMR analysis of complex mixtures. *Prog Nucl Mag Reson Spectr* **28:** 161–219

Floch MH (2002) Bile salts, intestinal microflora and enterohepatic circulation. *Dig Liver Dis* **34** (Suppl 2)**:** S54–S57

Fukushima M, Akiba S, Nakano M (1996) Comparative hypocholesterolemic effects of six vegetable oils in cholesterol-fed rat. *Lipids* **31:** 415–419

Fukushima M, Matsuda T, Yamagishi K, Nakano M (1997) Comparative hypocholesterolemic effects of six dietary oils in cholesterol-fed rats after long-term feeding. *Lipids* **32:** 1069–1074

Fuller R (2004) Probiotics in man and animals. *J Appl Bacteriol* **66:** 365–378

Gavaghan McKee CL, Wilson ID, Nicholson JK (2006) Metabolic phenotyping of nude and normal (Alpk:ApfCD, C57BL10J) mice. *J Proteome Res* **5:** 378–384

Gill SR, Pop M, Deboy RT, Eckburg PB, Turnbaugh PJ, Samuel BS, Gordon JI, Relman DA, Fraser-Liggett CM, Nelson KE (2006) Metagenomic analysis of the human distal gut microbiome. *Science* **312:** 1355–1359

Goodwin BL, Ruthven CR, Sandler M (1994) Gut flora and the origin of some urinary aromatic phenolic compounds. *Biochem Pharmacol* **47:** 2294–2297

Gunnarsson I, Andersson P, Wikberg J, Lundstedt T (2003) Multivariate analysis of G-protein-coupled receptors. *J Chemom* **17:** 82–92

Gupta P, Andrew H, Kirschner BS, Guandalini S (2000) Is *Lactobacillus* GG helpful in children with Crohn's disease? Results of a preliminary, open-label study. *J Pediatr Gastroenterol Nutr* **31:** 453–457

Hallson PC, Choong SK, Kasidas GP, Samuell CT (1997) Effects of Tamm-Horsfall protein with normal and reduced sialic acid content upon the crystallization of calcium phosphate and calcium oxalate in human urine. *Br J Urol* **80:** 533–538

Holmes E, Nicholson JK (2005) Variation in gut microbiota strongly influences individual rodent phenotypes. *Toxicol Sci* **87:** 1–2

Hurd RE (1990) Gradient-enhanced spectroscopy. *J Magn Reson* **87:** 422–428

Ibnou-Zekri N, Blum S, Schiffrin EJ, von der WT (2003) Divergent patterns of colonization and immune response elicited from two intestinal *Lactobacillus* strains that display similar properties *in vitro*. *Infect Immun* **71:** 428–436

Ikram-ul H, Mukhtar H (2006) Biosynthesis of protease from *Lactobacillus paracasei*: kinetic analysis of fermentation parameters. *Indian J Biochem Biophys* **43:** 377–381

Janne K, Pettersen J, Lindberg NO, Lundstedt T (2001) Hierarchical principal component analysis (PCA) and projection to latent structure (PLS) technique on spectroscopic data as a data pretreatment for calibration. *J Chemometr* **15:** 203–213

Jenkins JK, Courtney PD (2003) *Lactobacillus* growth and membrane composition in the presence of linoleic or conjugated linoleic acid. *Can J Microbiol* **49:** 51–57

Kajander K, Hatakka K, Poussa T, Farkkila M, Korpela R (2005) A probiotic mixture alleviates symptoms in irritable bowel syndrome patients: a controlled 6-month intervention. *Aliment Pharmacol Ther* **22:** 387–394

Kankaanpaa P, Yang B, Kallio H, Isolauri E, Salminen S (2004) Effects of polyunsaturated fatty acids in growth medium on lipid composition and on physicochemical surface properties of lactobacilli. *Appl Environ Microbiol* **70:** 129–136

Kishinaka M, Umeda A, Kuroki S (1994) High concentrations of conjugated bile acids inhibit bacterial growth of *Clostridium perfringens* and induce its extracellular cholylglycine hydrolase. *Steroids* **59:** 485–489

Kunz C, Rudloff S, Baier W, Klein N, Strobel S (2000) Oligosaccharides in human milk: structural, functional and metabolic aspects. *Annual review of nutrition* **20:** 699–722

Kurdi P, van Veen HW, Tanaka H, Mierau I, Konings WN, Tannock GW, Tomita F, Yokota A (2000) Cholic acid is accumulated spontaneously, driven by membrane deltapH, in many lactobacilli. *J Bacteriol* **182:** 6525–6528

Lederberg J (2000) Infectious history. *Science* **288:** 287–293

Ley R, Turnbaugh P, Klein S, Gordon J (2006) Microbial ecology: human gut microbes associated with obesity. *Nature* **444:** 1022–1023

Lin Y, Havinga R, Schippers IJ, Verkade HJ, Vonk RJ, Kuipers F (1996) Characterization of the inhibitory effects of bile acids on very-low-density lipoprotein secretion by rat hepatocytes in primary culture. *Biochem J* **316** (Part 2)**:** 531–538

Lundstedt T, Seifert E, Abramo L, Thelin B, Nystrom A, Pettersen J, Bergman R (1998) Experimental design and optimization. *Chemom Intell Lab Syst* **42:** 3–40

Macfarlane GT, Gibson GR, Beatty E, Cummings JH (1992) Estimation of short-chain fatty-acid production from protein by human intestinal bacteria based on branched-chain fatty-acid measurements. *FEMS Microbiol Ecol* **101:** 81–88

Mackie RI, Sghir A, Gaskins HR (1999) Developmental microbial ecology of the neonatal gastrointestinal tract. *Am J Clin Nutr* **69:** 1035S–1045S

Marchesi JR, Holmes E, Khan F, Kochhar S, Scanlan P, Shanahan F, Wilson ID, Wang Y (2007) Rapid and noninvasive metabonomic characterization of inflammatory bowel disease. *J Proteome Res* **6:** 546–551

Marshall B (2003) Helicobacter pylori: past, present and future. *Keio J Med* **52:** 80–85

Martin FP, Dumas ME, Wang Y, Legido-Quigley C, Yap IK, Tang H, Zirah S, Murphy GM, Cloarec O, Lindon JC, Sprenger N, Fay LB, Kochhar S, van BP, Holmes E, Nicholson JK (2007a) A top-down systems biology view of microbiome-mammalian metabolic interactions in a mouse model. *Mol Syst Biol* **3:** 112

Martin FP, Verdu EF, Wang Y, Dumas ME, Yap IK, Cloarec O, Bergonzelli GE, Corthesy-Theulaz I, Kochhar S, Holmes E, Lindon JC, Collins SM, Nicholson JK (2006) Transgenomic metabolic interactions in a mouse disease model: interactions of *Trichinella spiralis* infection with dietary *Lactobacillus paracasei* supplementation. *J Proteome Res* **5:** 2185–2193

Martin FP, Wang Y, Sprenger N, Holmes E, Lindon JC, Kochhar S, Nicholson JK (2007b) Effects of probiotic *Lactobacillus paracasei*

Published online: January 15, 2008

treatment on the host gut tissue metabolic profiles probed via magic-angle-spinning NMR spectroscopy. *J Proteome Res* **6:** 1471–1481

Meiboom S, Gill D (1958) Modified spin-echo method for measuring nuclear relaxation times. *Rev Sci Instrum* **29:** 688–691

Metges CC (2000) Contribution of microbial amino acids to amino acid homeostasis of the host. *J Nutr* **130:** 1857S–1864S

Metges CC, Eberhard M, Petzke KJ (2006) Synthesis and absorption of intestinal microbial lysine in humans and non-ruminant animals and impact on human estimated average requirement of dietary lysine. *Curr Opin Clin Nutr Metab Care* **9:** 37–41

Midtvedt T, Norman A (1967) Bile acid transformations by microbial strains belonging to genera found in intestinal contents. *Acta Pathol Microbiol Scand* **71:** 629–638

Nicholson JK (2006) Global systems biology, personalized medicine and molecular epidemiology. *Mol Syst Biol* **2:** 52

Nicholson JK, Foxall PJ, Spraul M, Farrant RD, Lindon JC (1995) 750 MHz 1H and ^{1}H-^{13}C NMR spectroscopy of human blood plasma. *Anal Chem* **67:** 793–811

Nicholson JK, Holmes E, Lindon JC, Wilson ID (2004) The challenges of modeling mammalian biocomplexity. *Nat Biotechnol* **22:** 1268–1274

Nicholson JK, Holmes E, Wilson ID (2005) Gut microorganisms, mammalian metabolism and personalized health care. *Nat Rev Microbiol* **3:** 431–438

Nicholson JK, Wilson ID (2003) Opinion: understanding 'global' systems biology: metabonomics and the continuum of metabolism. *Nat Rev Drug Discov* **2:** 668–676

Nowak A, Libudzisz Z (2006) Influence of phenol, p-cresol and indole on growth and survival of intestinal lactic acid bacteria. *Anaerobe* **12:** 80–84

Ouwehand AC (2007) Antiallergic effects of probiotics. *J Nutr* **137:** 794S–797S

Pereira DI, Gibson GR (2002) Effects of consumption of probiotics and prebiotics on serum lipid levels in humans. *Crit Rev Biochem Mol Biol* **37:** 259–281

Pereira DI, McCartney AL, Gibson GR (2003) An *in vitro* study of the probiotic potential of a bile-salt-hydrolyzing *Lactobacillus fermentum* strain, and determination of its cholesterol-lowering properties. *Appl Environ Microbiol* **69:** 4743–4752

Rasic J (1992) Assimilation of cholesterol by some cultures of lactic-acid bacteria and bifidobacteria. *Biotechnol Lett* **14:** 39–44

Reeves PG, Nielsen FH, Fahey Jr GC (1993) AIN-93 purified diets for laboratory rodents: final report of the American Institute of Nutrition *ad hoc* writing committee on the reformulation of the AIN-76A rodent diet. *J Nutr* **123:** 1939–1951

Reid G, Bruce A (2006) Probiotics to prevent urinary tract infections: the rationale and evidence. *World J Urol* **24:** 28–32

Rezzi S, Ramadan Z, Fay LB, Kochhar S (2007) Nutritional metabonomics: applications and perspectives. *J Proteome Res* **6:** 513–525

Salminen SJ, Gueimonde M, Isolauri E (2005) Probiotics that modify disease risk. *J Nutr* **135:** 1294–1298

Sarker SA, Sultana S, Fuchs GJ, Alam NH, Azim T, Brussow H, Hammarstrom L (2005) *Lactobacillus paracasei* strain ST11 has no effect on rotavirus but ameliorates the outcome of nonrotavirus diarrhea in children from Bangladesh. *Pediatrics* **116:** e221–e228

Sartor RB (2004) Therapeutic manipulation of the enteric microflora in inflammatory bowel diseases: antibiotics, probiotics, and prebiotics. *Gastroenterology* **126:** 1620–1633

Sasaki M, Bosman BW, Tan PS (1995) Comparison of proteolytic activities in various lactobacilli. *J Dairy Res* **62:** 601–610

Scholz-Ahrens KE, Schaafsma G, van den Heuvel EG, Schrezenmeir J (2001) Effects of prebiotics on mineral metabolism. *Am J Clin Nutr* **73:** 459S–464S

Smith EA, Macfarlane GT (1996) Enumeration of human colonic bacteria producing phenolic and indolic compounds: effects of pH, carbohydrate availability and retention time on dissimilatory aromatic amino acid metabolism. *J Appl Bacteriol* **81:** 288–302

Smith JL, Wishnok JS, Deen WM (1994) Metabolism and excretion of methylamines in rats. *Toxicol Appl Pharmacol* **125:** 296–308

Szynanski H, Pejcz J, Jawien M, Chmielarczyk A, Strus M, Heczko P (2006) Treatment of acute infectious diarrhoea in infants and children with a mixture of three *Lactobacillus rhamnosus* strains—a randomized, double-blind, placebo-controlled trial. *Aliment Pharmacol Ther* **23:** 247–253

Taranto MP, Fernandez Murga ML, Lorca G, De Valdez GF (2003) Bile salts and cholesterol induce changes in the lipid cell membrane of *Lactobacillus reuteri*. *J Appl Microbiol* **95:** 86–91

Trygg J, Wold S (2003) O2-PLS, a two-block (X-Y) latent variable regression (LVR) method with an integrated OSC filter. *J Chemom* **17:** 53–64

Turnbaugh P, Ley R, Mahowald M, Magrini V, Mardis E, Gordon J (2006) An obesity-associated gut microbiome with increased capacity for energy harvest. *Nature* **444:** 1027–1031

Verdu EF, Bercik P, Bergonzelli GE, Huang XX, Blennerhasset P, Rochat F, Fiaux M, Mansourian R, Corthesy-Theulaz I, Collins SM (2004) *Lactobacillus paracasei* normalizes muscle hypercontractility in a murine model of postinfective gut dysfunction. *Gastroenterology* **127:** 826–837

Wang Y, Lawler D, Larson B, Ramadan Z, Kochhar S, Holmes E, Nicholson JK (2007) Metabonomic investigations of aging and caloric restriction in a life-long dog study. *J Proteome Res* **6:** 1846–1854

Wang Y, Tang H, Holmes E, Lindon JC, Turini ME, Sprenger N, Bergonzelli G, Fay LB, Kochhar S, Nicholson JK (2005) Biochemical characterization of rat intestine development using high-resolution magic-angle-spinning ^{1}H NMR spectroscopy and multivariate data analysis. *J Proteome Res* **4:** 1324–1329

Warren JR (2000) Gastric pathology associated with Helicobacter pylori. *Gastroenterol Clin North Am* **29:** 705–751

Watanabe M, Houten SM, Wang L, Moschetta A, Mangelsdorf DJ, Heyman RA, Moore DD, Auwerx J (2004) Bile acids lower triglyceride levels via a pathway involving FXR, SHP, and SREBP-1c. *J Clin Invest* **113:** 1408–1418

Waters NJ, Garrod S, Farrant RD, Haselden JN, Connor SC, Connelly J, Lindon JC, Holmes E, Nicholson JK (2000) High-resolution magic angle spinning ^{1}H NMR spectroscopy of intact liver and kidney: optimisation of sample preparation procedures and biochemical stability of tissue during spectral acquisition. *Anal Biochem* **282:** 16–23

Westerhuis JA, Kourti T, MacGregor JF (1998) Analysis of multiblock and hierarchical PCA and PLS models. *J Chemometr* **12:** 301–321

Wold S, Esbensen K, Geladi P (1987) Principal component analysis. *Chemometr Intell Lab Syst* **2:** 37–52

Wong JM, de Souza R, Kendall CW, Emam A, Jenkins DJ (2006) Colonic health: fermentation and short chain fatty acids. *J Clin Gastroenterol* **40:** 235–243

Xu S, Boylston TD, Glatz BA (2005) Conjugated linoleic acid content and organoleptic attributes of fermented milk products produced with probiotic bacteria. *J Agric Food Chem* **53:** 9064–9072

Xu ZR, Hu CH, Wang MQ (2002) Effects of fructooligosaccharide on conversion of L-tryptophan to skatole and indole by mixed populations of pig fecal bacteria. *J Gen Appl Microbiol* **48:** 83–90

Zeisel SH, Wishnok JS, Blusztajn JK (1983) Formation of methylamines from ingested choline and lecithin. *J Pharmacol Exp Ther* **225:** 320–324

Published online: January 15, 2008